Generalized Back Projection Algorithm Based on Node Analysis in 3-D EIT

Hongbin Wang[1], Guizhi Xu[1], Ying Li[1], Weili Yan[1]
[1] Province-Ministry Joint Key Laboratory of Electromagnetic Field and Electrical Apparatus Reliability, Hebei University of Technology, Tianjin 300130, P.R. China
E-mail: wanghongbin369@163.com

Abstract

In this paper, we propose a new algorithm named generalized back projection algorithm via node analysis (GBPA-NA), with purpose of solving low resolution problem in electrical impedance tomography (EIT) reconstruction images. The new method calculates projection matrix in integral form instead of differential form, so that the reconstructed images resolution is improved for residual error reduced. GBPA-NA is applied to image reconstruction using a simulation cylinder model and real experimental model of 128-channel EIT system respectively. The results indicate that the quality of images reconstructed by GBPA-NA is better than that of the previous back-projection-based algorithms accessed by four metrics. The proposed method is promising in clinic feasibly.

Keywords: Electrical impedance tomography, Generalized Back Projection Algorithm, Image evaluation

1. Introduction

Electrical Impedance Tomography (EIT) is a subject of much recent interest, which attempts to estimate the impedance distribution inside an object from electrical measurements on its surface [1-2]. Back projection algorithm (BPA) is a typical dynamic image reconstruction algorithm in EIT [3]. This algorithm calculates data collected at different moments, so that reconstructed results are represented to differential images with low noise information. However, BPA don't perform so well for information loss during the projection process. The very reason is subdivision, in which process the much internal information of elements is ignored. In [4], we proposed Generalized Back Projection Algorithm (GBPA), which expands the area of computation objects to arbitrary part in subject.

GBPA bases on linearised sensitivity relationship [5], in which computation process the curl of potential should be calculated. Thus the potential fitting function in forward problem is required derivable. In practice, high variation at boundary of organs or tumors leads to difficulty of potential function fitting. The fact may hardly represent to a continuous and derivable function, or the very deviation may exist in the fitting function. So the residual error results in low resolution, which remains in reconstruction results.

In this paper we present a new method based on GBPA, which calculates projection matrix by node analysis. In EIT problem, the resistance perturbation is proportional to the curl of potential variation. According to this relationship, we establish a coordinate system at boundary to describe projection position. Thus we get calculation formula of the resistance perturbation as an integration of the potential function corresponding to boundary coordinate system, instead of the curl of the potential function.

2. Method

In EIT, computational region Ω can be treated as a quasi-static field. If we consider the general form of Ohm's law for a point within an Ohmic conductor, expressing the electric field E in terms of the electric potential φ, we have

$$\rho = -J^{-1}\nabla\varphi \tag{1}$$

where conductivity σ is replace by resistivity ρ.

If we assume equi-potential line to a circuit, the sum of the current through the line can be considered an excited current source, and the equivalent normal resistivity ρ is the sum of each part on the equi-potential line [6]. Since the potential function in one element can be determined through finite element method (FEM), we assume imaginary elements are substituted for previous subdivision elements to describe the assumed circuit accurately.

At the original moment t_0, the potential of an imaginary node can be calculated through potential function ϕ of FEM and the potential of the element nodes. Then the potential distribution φ_0 is

$$\varphi_0 = \int \tilde{\varphi} d\Omega = \int \phi^{-1}\left(\varphi_0^j\right) d\Omega \tag{2}$$

where j corresponds to the j^{th} imaginary element.

To describe the projection position, we establish a coordinate system on object boundary. The node potential can map to the boundary voltage distribution.

$$\varphi(x) = \int J\tilde{\rho}(x) dx \tag{3}$$

where x denotes coordinate value, i.e. the mapping position in boundary plane.

Write (3) in differential form, then substituting it into (1), the variation from moment t_0 to t_1 is

$$\Delta\tilde{\rho} = -J^{-1} \frac{d\left(\varphi_1 - \int \phi^{-1}\left(\varphi_0^j\right) d\Omega\right)}{dx} \tag{4}$$

If the boundary voltage curve can be fitted by polynomial, we have

$$\Delta\tilde{\rho} = -J^{-1} \sum_{i=1}^{n} \left(q_i - \int \phi^{-1}\left(p_i^j\right) d\Omega\right)(n+1-i)x^{n-i} \tag{5}$$

where n is the order of polynomial, p_i and q_i $(i = 1,2,\cdots,n+1)$ is the coefficient of polynomials.

3. Numerical Simulation and Evaluation

As shown in Fig. 1 (a), the simulation cylinder is established to assess the performance of GBPA. The resistivity of targets is assumed to be $3\,\Omega\cdot\mathrm{m}$, and the other to be $2\,\Omega\cdot\mathrm{m}$. The four-plane simultaneous adjacent drive-receive electrode configuration is arranged in the simulation. The reconstructed results are shown in Fig. 2.

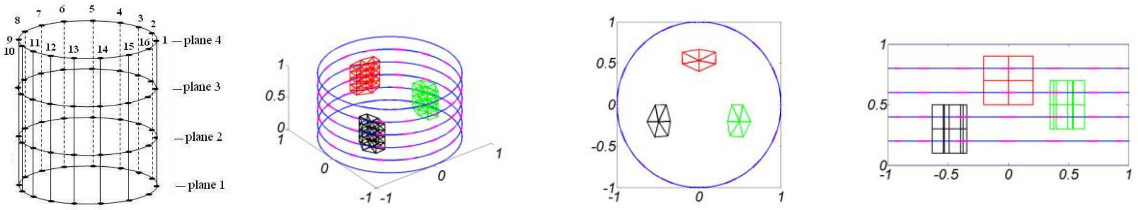

(a) Electrode array (b) Lateral view (c) Top view (d) Front view

Fig. 1. Three views of 3D cylinder model with three targets

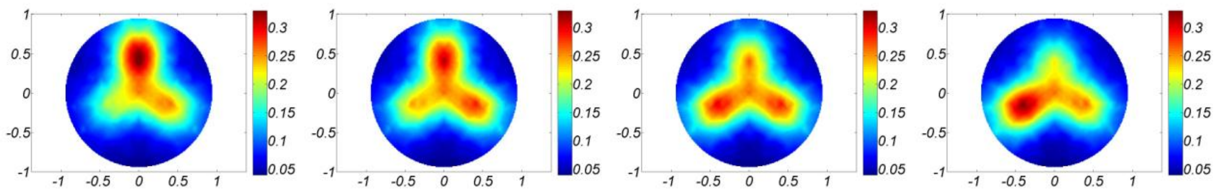

(a) Section 4 (b) Section 3 (c) Section 2 (d) Section 1

Fig. 2. Reconstructed results of simulation model

To quantitatively interpret the reconstruction results, we use four metrics in [4] referencing [7]. We calculate a target object set $\hat{x}_s$, which contains all image pixels $[\hat{x}]_i$ greater than 75% of the maximum amplitude p. The centre of gravity (CoG) of $\hat{x}$ and $\hat{x}_s$ are calculated, and the distance from the CoG of reconstructed targets to the default targets centre is then calculated. Based on images of point targets, we use the following parameters:

(1) Position error (PE) measures the extent to which the position of target is faithfully reconstructed.

$$PE = \frac{1}{k} \sum_{s=1}^{k} p_s (r_t - r_s) \tag{6}$$

where r_t is the CoG of default targets, r_s is the pixel position of the reconstructed target object set s, and k is the pixel number in this set. PE should be small and show small variability for targets at different radial positions.

(2) Resolution (RES) measures the size of reconstructed targets as a fraction of the medium.

$$RES = \sqrt{\sum_k p[\hat{x}_s]_k \Big/ \sum_{i\in\Omega} p[\hat{x}]_i} \tag{7}$$

RES should be small in order to more accurately represent the shape of the target conductivity distribution. Low value of RES serves primarily to distinguish nearby targets.

(3) Shape deformation (SD) measures the fraction of the reconstructed pixel set which does not fit within a circle specified for targets.

$$SD = \sum_{k\notin T} p[\hat{x}_s]_k \Big/ \sum_k p[\hat{x}_s]_k \tag{8}$$

where T is a circle which is centred at the CoG of $\hat{x}_s$ with an area equivalent to p_s. Large SD may result in incorrect interpretation of images.

(4) Information Entropy (IE) measures the information amount of the reconstructed images.

$$IE = \sum_i \left(\left(p[\hat{x}]_i \Big/ \sum p[\hat{x}] \right) \ln\left(p[\hat{x}]_i \Big/ \sum p[\hat{x}] \right) \right) \tag{9}$$

where we choose the ratio of any pixel amplitude and the sum of pixels amplitude. Large IE means more reconstructed information contained to provide more help to diagnosis.

In order to compare conventional Back Projection Algorithm (BPA), Node Back Projection Algorithm (NBPA) [6] and GBPA based on linearised sensitivity relationship (GBPA-LSR) [4] with GBPA via node analysis (GBPA-NA), the four parameters are computed and showed in TABLE I.

TABLE I. COMPARISON OF BPA NPBA GBPA-LSR AND GBPA-NA

	PE	RES	SD	IE
BPA	0.35006	0.48304	0.32954	40.302
NBPA	0.34546	0.42007	0.31925	40.467
GBPA-LSR	0.33573	0.41751	0.31573	40.493
GBPA-NA	0.33447	0.40968	0.31033	40.529

From TABLE I., the comparison results between the new method and other projection algorithms indicate reconstruction capability of GBPA is better than those of the others.

4. Experimental Results

The experimental phantom is designed with a diameter of 30 cm and height of 30 cm. As shown in Fig. 4. (a), the 16×4 electrode array is attached to the side surface of the phantom with 16 electrodes in each plane [8].

Plexiglas rod is placed upright on the bottom of phantom, which length is 18 cm and diameter is 2.5 cm. We adopt the injection strategy same as that in simulation experiment, getting reconstructed images as shown in Fig. 4. The reconstructed target is clearly recognizable.

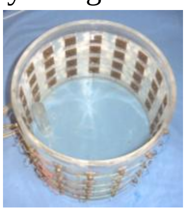

(a) Experimental mode

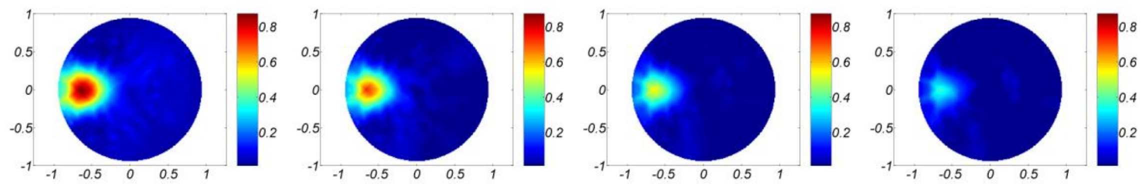

(b) Section 4 (c) Section 3 (d) Section 2 (e) Section 1

Fig. 4. Reconstructed results of experimental phantom

5. Conclusion

In this paper, we have introduced the improved GBPA via node analysis. The new method calculates projection matrix in integral form instead of differential form, so that residue error from conductivity distribution distortion can be avoided to some extent. The simulation experiment results indicate the proposed method performs well. According to the four metrics, the images reconstructed by GBPA-NA illustrate the targets more distinguished and accurate. In real experiment, we observed the reconstruction ability of the proposed method. The spatial resolution of reconstructed images further demonstrates that GBPA-NA can help to improve the accuracy of locating and shape determining. For further work, efforts will be on reducing artifacts, so that the new method could be helpful to diagnose in clinical.

Acknowledgements

This work was supported in part by the National Natural Science Foundation of China under Grant No. 50937005 and No. 51077040, and the Natural Science Foundation of Hebei province, CHINA under Grant No.E2011202026.

References

[1] Brown B. H. 2003 Electrical Impedance Tomography (EIT): a review *J. Med. Eng. Technol.* 27 97-108

[2] Lionheart W R 2004 EIT Reconstruction Algorithms: Pitfalls, Challenges and Recent Developments *Physiol. Meas.* 25 125-142

[3] Brown B. H., Seagar A. D. 1987 The Sheffield data collection system *Clin. Phys. Physio.* 8 91-97

[4] Wang Hongbin, Xu Guizhi, Zhang Shuai, et al 2011 Implementation of Generalized Back Projection Algorithm in 3-D EIT *IEEE Transactions on Magnetics* 47(5) 1466-1469

[5] Barber D C 1990 Image Reconstruction in Applied Potential Tomography – Electrical Impedance Tomography *Internal Report* Department of Medical Physics and Clinical Engineering, University of Sheffield, UK

[6] Zhang Jianjun, Yan Weili, Xu Guizhi, et al 2007 A New Algorithm to Reconstruct EIT Images: Node-Back-Projection Algorithm *IEEE EMBC 2007, 29th Annual International Conference, France* 4390-4393.

[7] Adler A, Arnold J H, Bayford R, et al 2009 GREIT: a unified approach to 2D linear EIT reconstruction of lung images *Physiol. Meas.* 30 S35-S55

[8] Xu Guizhi, Wang Renping, Zhang Shuai, et al 2007 A 128-Electrode Three Dimensional Electrical Impedance Tomography System *IEEE EMBC 2007, 29th Annual International Conference, France* 4386-4389